2004

Single-mode simulations of a short Rayleigh length FEL

Colson, W.B.

Nuclear Instruments and Methods in Physics Research A, Volume 528, (2004), pp. 167Ã¢ 171
http://hdl.handle.net/10945/44080

Available online at www.sciencedirect.com
SCIENCE DIRECT®
ELSEVIER
Nuclear Instruments and Methods in Physics Research A 528 (2004) 167–171
NUCLEAR INSTRUMENTS & METHODS IN PHYSICS RESEARCH
Section A
www.elsevier.com/locate/nima

Single-mode simulations of a short Rayleigh length FEL

W.B. Colson*, J. Blau, R.L. Armstead, P.P. Crooker

Physics Department, Naval Postgraduate School, Monterey, CA 93943, USA

Abstract

Free electron lasers can make use of a short Rayleigh length optical mode in order to reduce the intensity on resonator mirrors. A simulation method is used that includes the dynamics of this rapidly focusing optical mode and the macroscopic and microscopic electron evolution. The amplitude and phase of the optical fields are represented by a single Gaussian mode. The simulation runs in seconds on small laptop computers and can be used for system analysis. Published by Elsevier B.V.

PACS: 41.60Cr

Keywords: Free electron laser; Short Rayleigh length

1. Introduction

In a high-power free electron laser (FEL), a short Rayleigh length resonator can be used to reduce the optical intensity on the mirrors. Typically, the short optical Rayleigh length requires the use of a short undulator so that the expanding optical beam does not scrape power on the magnets. This paper develops a simple simulation model that describes the energy extraction in a high-power FEL using a short Rayleigh length optical mode with a deterministic form that tracks the rapid diffraction of the laser beam. Thousands of sample electrons interact with the laser field in the middle of the rapidly diffracting wave front. The simulation method can be used over a wide range of parameters to study FEL characteristics more efficiently.

2. The optical mode

The optical mode in an FEL is determined by the electron beam interaction, diffraction, and by the resonator mirrors. In most FEL oscillators, it has been observed that more than 90% of the optical power remains in the fundamental mode at saturation where the gain is reduced to equal the resonator output coupling $\alpha_n = 1/Q_n$. Higher-order modes have little impact on the far-field limit and the FEL interaction. The optical electric field in the fundamental mode [1] is

$$E(r, z) = E_0(\lambda Z_0/A)^{1/2}\, e^{i(kz-\omega t+\phi)} \exp(-\pi r^2/A) \quad (1)$$

*Corresponding author. Tel.: +1-831-656-2765.
E-mail address: colson@nps.edu (W.B. Colson).

0168-9002/$ - see front matter Published by Elsevier B.V.
doi:10.1016/j.nima.2004.04.039

where $\phi(r,z) = -\tan^{-1}[(z-z_w)/Z_0] + \pi r^2(z-z_w)/AZ_0$ is the optical phase, $A = \lambda Z_0[1+(z-z_w)^2/Z_0^2]$ is the optical mode area, $\lambda = 2\pi/k$ is the FEL optical wavelength, k is the optical wave number, ω is the optical frequency, z is the position along the undulator ($z = 0$ at the beginning, $z = L$ at the end of the undulator), r is the radial position in the mode, z_w is the position of the optical mode waist, Z_0 is the mode's Rayleigh length, and E_0 is the optical electric field amplitude at the mode waist $z = z_w$. The optical electric field is determined by the intra-cavity power, and is given by $E_0^2 = (8\pi Q_n P_{out})/(cZ_0\lambda D_{duty})$ where the FEL average output power is P_{out}, the laser beam duty factor is $D_{duty} = l_b\Omega/c$, l_b is the electron micropulse length, Ω is the pulse repetition frequency, and c is the speed of light [2].

3. The electron beam

The electron beam's initial energy is $E_b = \gamma_0 mc^2$ with a Lorentz factor of γ_0, where m is the electron mass. A realistic beam has a small spread in energies, but in the short undulator this is generally of no consequence. Each micropulse of electrons contains charge q with a repetition frequency of Ω, giving an average electron beam current of $I_{av} = q\Omega$. The average power flowing in the electron beam is $P_b = I_{av}E_b/e$ where e is the electron charge magnitude.

The electron beam's waist radius is r_b at the beam focus, located along the undulator at z_b. A sample electron's initial transverse positions (x_0, y_0) and angles (θ_x, θ_y) are distributed as Gaussians. Consistent with the normalized beam emittance, $\varepsilon_n = \gamma_0 r_b \theta_b$, the resulting electron beam's angular spread is θ_b. For simplicity, the beam is taken to be round here, but the simulation can handle beam asymmetries in x and y. There is no significant betatron focusing in the short undulator, so the electron's injection angles remain constant along the undulator in each direction. An electron's transverse position at distance z along the undulator is given by $x(z) = x_0 + \theta_x(z - z_b)$ and $y(z) = y_0 + \theta_y(z - z_b)$. The laser interaction does not affect the transverse positions of the electrons, but their transverse positions significantly affect the electron's microscopic longitudinal position, and therefore bunching, energy extraction, and gain.

4. The FEL interaction

An electron's interaction with the transverse fields of the laser light is made possible by passing the beam through the transverse fields of the undulator. The undulator field is linearly polarized with the form $\mathbf{B} = B(0, \sin k_0 z, 0)$ on the undulator axis where the electrons travel. The peak magnetic field in the undulator is B, and the undulator period is $\lambda_0 = 2\pi/k_0$. The electron's transverse motion in the undulator is $\boldsymbol{\beta}_\perp = -(\sqrt{2}K/\gamma)(\cos k_0 z, 0, 0)$ where the undulator parameter is $K = eB\lambda_0/(2\sqrt{2}\pi mc^2)$, and the electron's velocity is $\mathbf{v} = c\boldsymbol{\beta}$. The linearly polarized electric and magnetic optical fields describing the optical mode above are $\mathbf{E}_s = E(\cos\psi, 0, 0)$, $\mathbf{B}_s = E(0, \cos\psi, 0)$ where $\psi = kz - \omega t + \phi$, and the optical mode's amplitude E and phase ϕ are given earlier. Substituting $\boldsymbol{\beta}_\perp$, $\mathbf{E}_s$, and $\mathbf{B}_s$ into the Lorentz force equations, an electron's Lorentz factor, $\gamma = (1 - \boldsymbol{\beta}^2)^{-1/2}$, evolves according to

$$\gamma' = (eKE/\gamma mc^2)[J_0(\xi) - J_1(\xi)]\cos(\zeta + \phi) \tag{2}$$

where J_0 and J_1 are Bessel functions, $\xi = K^2/2(1+K^2)$, $\zeta = (k+k_0)z - \omega t$ is the electron phase, $\gamma' = \mathrm{d}\gamma/\mathrm{d}z$, and integration along the undulator is in small steps $\mathrm{d}z$ instead of time, using $\mathrm{d}z = c\mathrm{d}t$. "Fast" longitudinal motion in the linearly polarized undulator has been averaged away, giving rise to the Bessel function factors $J_0(\xi) - J_1(\xi)$ [3]. During the integration of the dynamic Lorentz factor $\gamma(z)$ along the undulator, $z = 0 \to L$, the optical mode's amplitude E and phase ϕ and the electron's transverse positions, x and y, are simply evaluated at each step. The evolution of the electron phase $\zeta = (k+k_0)z - \omega t$ is crucial to FEL performance, and describes electron bunching, gain, and extraction [4].

The electron phase ζ is a microscopic variable measuring the electron position on the optical wavelength scale. The initial electron phases ζ_0 are uniformly spread over a 2π range. When there is no interaction ($\gamma' = d\gamma/dz = 0$, $\gamma = \gamma_0$), the electron phase is determined by $\zeta' = \nu_0/L$ where the initial electron phase velocity is $\nu_0 = L[(k + k_0)\beta_z(0) - k]$ and $c\beta_z(0)$ is the electron's initial velocity. Integration gives $\zeta = \zeta_0 + z\nu_0/L$. When there is an interaction ($\gamma' \neq 0$), the Lorentz factor $\gamma(z)$ evolves by integrating γ' in (2) including self-consistent changes in the electron phase determined by $\zeta' = [\nu_0 + 4\pi N(\gamma - \gamma_0)/\gamma_0]/L$.

The simulation uses a large number of sample electrons, ranging from 10^3 to 10^4 as more are needed for a larger radial spread r_b. After integration of all the sample electrons through the undulator length ($z = 0 \to L$ in a few hundred small steps dz), the electron beam's extraction is given by $\eta = \langle \gamma_0 - \gamma \rangle / \gamma_0$ where $\langle \ldots \rangle$ is an average over the sampled electrons. If the self-consistent changes in ζ are not included above, $\langle \ldots \rangle$ and η are always zero. In an FEL oscillator, the optical wavelength evolves freely to the value for maximum gain in weak optical fields, or maximum energy extraction in strong optical fields at saturation. The waveform described by E and ϕ above has a single, fixed wavelength that determines the value of the initial phase velocity ν_0. The simulation searches through values of ν_0 (typically from $\nu_0 = 0$ to 16) and finds the maximum extraction η (typically around $\nu_0 = 8{-}9$). At the best value of ν_0 found, the simulation calculates the FEL's final extraction and the resulting output optical power $P_{calc} = P_b\eta$. The value of the optical power that would lead to steady-state saturation can be determined by iteration. At the end of each iteration, the calculated output power is used as the input for the next iteration. If the initial power is above or below the steady-state value, it decreases or increases appropriately over a few iterations until the stable, steady-state power is found.

5. Simulation results

As an example, take the initial electron beam energy to be $E_b \approx 100$ MeV ($\gamma_0 \approx 197$) with micropulse peak current $I_{peak} \approx 1500$ A, micropulse length $l_b \approx 0.3$ mm (1 ps duration), micropulse

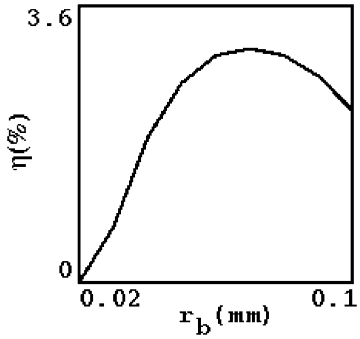

Fig. 1. The FEL extraction $\eta(r_b)$ shows optimum electron beam focal radius r_b.

charge $q \approx 1.5$ nC, electron beam radius $r_b \approx 70$ μm at the beam focus $z_b = 0.5L$, and normalized emittance $\varepsilon_n \approx 9$ mm-mradians. The undulator has $N = 14$ periods each of length $\lambda_0 \approx 2.7$ cm (total length $L \approx 37$ cm) with undulator parameter $K \approx 1.4$ resulting in optical wavelength $\lambda \approx 1$ μm. Resonator mirrors have an output coupling of $\alpha_n = 1/Q_n \approx 50\%$ ($Q_n \approx 2$), and their curvature determines the Rayleigh length $Z_0 \approx 2.6$ cm, dimensionless Rayleigh length $z_0 = Z_0/L \approx 0.07$, creating an optical mode waist $w_0 \approx 90$ μm at the center of the undulator $\tau_w = 0.5L$.

Fig. 1 shows the FEL extraction $\eta(r_b)$ as the electron beam focal radius is varied from $r_b = 0.02$ mm up to $r_b = 0.1$ mm with fixed emittance ε_n. As r_b is increased from 0.02 mm, the optical output increases from $\eta \approx 0$ extraction to a peak of $\eta \approx 3.1\%$ at $r_b = 0.07$ mm. As the electron beam focal radius is increased further from $r_b = 0.07$ mm to 0.1 mm, the extraction decreases to $\eta \approx 2.3\%$. At large focal radius near $r_b = 0.1$ mm, some of the electron beam is outside the optical waist radius $w_0 \approx 0.09$ mm, thereby reducing the extraction. For a small focal radius near $r_b = 0.02$ mm, the increased angular spread causes some of the beam to diverge outside the optical mode at each end of the undulator. The balance of these two competing effects gives an optimum electron beam focal radius of $r_b \approx 0.07$ mm for these parameters.

Fig. 2 shows the FEL extraction $\eta(z_0)$ as the dimensionless Rayleigh length is varied from $z_0 =$

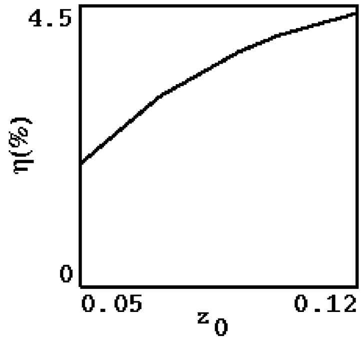

Fig. 2. The FEL extraction $\eta(z_0)$ increases monotonically with increasing Rayleigh length z_0.

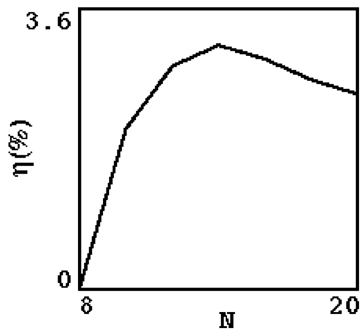

Fig. 3. The FEL extraction $\eta(N)$ shows an optimum number of undulator periods N.

0.05 to 0.12, corresponding to actual Rayleigh lengths $Z_0 = 1.85$ cm to $Z_0 = 4.44$ cm ($Z_0 = Lz_0$). A smaller Rayleigh length increases the mode area on the mirrors, but reduces the electron–optical interaction because of the rapidly changing optical phase, rapidly changing optical amplitude, and short interaction length. For a small Rayleigh length of $z_0 = 0.05$, the extraction is only $\eta \approx 2\%$. As z_0 increases to 0.12, the extraction increases to $\eta \approx 4.5\%$. The extraction steadily increases with z_0, but mirror intensity increases rapidly for two reasons: (i) the increasing extraction, and (ii) the decreasing mode area at the mirrors. The lower values of z_0 significantly reduce the intensity on the mirrors with only a small reduction in the FEL energy extraction η.

Fig. 3 shows the FEL extraction $\eta(N)$ as the number of undulator period is varied from $N = 8$ to 20. With a short Rayleigh length ($Z_0 \ll L$), the optical mode expands significantly along even the shortest undulator and care must be taken that the laser energy "scraped" off the optical beam does not heat or damage the undulator walls. For all the values examined here, the scraped energy remains small (less than a Watt) for an undulator gap of 1 cm. For a shortest undulator of $N = 8$ periods, the interaction length is so small that the FEL is below threshold (output/pass exceeds gain/pass), and extraction is zero. As N increases, the extraction increases to a peak value of $\eta = 3\%$ at $N = 14$ periods. At larger values of N, the extraction decreases slightly down to $\eta = 2.5\%$ at $N = 20$ periods. After reaching the optimum undulator length, there is no further advantage in increasing the undulator length. In fact, there is a penalty since the FEL extraction tends to decrease with increasing N.

6. Conclusions

A simulation method, capturing the important physics of the short Rayleigh length FEL, has been described. The method is then used to explore FEL energy extractions $\eta(r_b)$, $\eta(z_0)$, and $\eta(N)$. The extraction $\eta(r_b)$ shows an optimum electron beam focal radius r_b. A more accurate determination of the optimum value for r_b should be obtained by more sophisticated simulations, or better yet, experiments. Increasing values of the Rayleigh length z_0 steadily improves the FEL interaction and single-pass extraction $\eta(z_0)$, but focuses the power to a smaller mirror spot that can exceed the damage limit. The extraction $\eta(N)$ increases rapidly with N up to an optimum value. Further increases in the undulator length do not improve the interaction because of the diminished optical field strength at both ends of the undulator.

Acknowledgements

The authors are grateful for the support from NAVSEA and the JTO.

References

[1] A. Yariv, Quantum Electronics, Wiley, New York, 1975, p. 112 (Chapter 6).
[2] J.D. Jackson, Classical Electrodynamics, Wiley, New York, 1962, p. 205.
[3] W.B. Colson, G. Dattoli, F. Ciocci, Phys. Rev. A 31 (1985) 828.
[4] W.B. Colson, C. Pellegrini, A. Renieri (Eds.), Free Electron Laser Handbook, North-Holland Physics, Elsevier Science Publishing Co. Inc., The Netherlands, 1990 (Chapter 5).